HHS Public Access

Author manuscript

Biochim Biophys Acta. Author manuscript; available in PMC 2015 April 02.

Published in final edited form as:

Biochim Biophys Acta. 2013 June ; 1830(6): 3828–3834. doi:10.1016/j.bbagen.2013.02.015.

Effect of Lyso-phosphatidylcholine and Schnurri-3 on Osteogenic Transdifferentiation of Vascular Smooth Muscle Cells to Calcifying Vascular Cells in 3D Culture

Fernando Castro-Chavez[a], **Kasey C. Vickers**[a], **Jae Sam Lee**[b], **Ching-Hsuan Tung**[b], and **Joel D. Morrisett**[a,*]

[a]Department of Medicine, Atherosclerosis and Vascular Medicine Section, Methodist DeBakey Heart Center, Baylor College of Medicine, Houston, TX, USA

[b]Department of Radiology, The Methodist Hospital Research Institute, Weill Cornell Medical College, Houston, TX, USA

Abstract

Background—In vitro cell culture is a widely used technique for investigating a range of processes such as stem cell behavior, regenerative medicine, tissue engineering, and drug discovery. Conventional cell culture is performed in Petri dishes or flasks where cells typically attach to a flat glass or plastic surface as a cell monolayer. However, 2D cell mono-layers do not provide a satisfactory representation of in vivo conditions. A 3D culture could be a much better system for representing the conditions that prevail in vivo.

Methods and results—To simulate 3D conditions, vascular smooth muscle cells (VSMCs) were loaded with gold–polyvmer–iron oxide hydrogel, enabling levitation of the cells by using spatially varying magnetic fields. These magnetically levitated 3D cultures appeared as freely suspended, clustered cells which proliferated 3–4 times faster than cells in conventional 2D cultures. When the levitated cells were treated with 10 nM lysophosphatidylcholine (LPC), for 3 days, cell clusters exhibited translucent extensions/rods 60–80 μm wide and 200–250 μm long. When 0.5 μg/μl Schnurri-3 was added to the culture containing LPC, these extensions were smaller or absent. When excited with 590–650 nm light, these extensions emitted intrinsic fluorescence at >667 nm. When the 3D cultures were treated with a fluorescent probe specific for calcium hydroxyapatite (FITC-HABP-19), the cell extensions/rods emitted intensely at 518 nm, the λ_{max} for FITC emission. Pellets of cells treated with LPC were more enriched in calcium, phosphate, and glycosaminogly-cans than cells treated with LPC and Schnurri-3.

Conclusions—In 3D cultures, VSMCs grow more rapidly and form larger calcification clusters than cells in 2D cultures. Transdifferentiation of VSMC into calcifying vascular cells is enhanced by LPC and attenuated by Schnurri-3.

*Corresponding author at: 6565 Fannin St,MS-A601, The Methodist Hospital, Houston, TX 77030, USA. Tel.: +1 713 798 4164; fax: +1 713 798 4121. morriset@bcm.edu (J.D. Morrisett).

Supplementary materials related to this article can be found online at doi:10.1016/j.bbagen.2013.02.015.

General significance—The formation of calcified structures in 3D VSMC cultures suggests that similar structures may be formed in vivo.

Keywords

Osteocalcin; Magnetic levitation; Calcifying cell; Atherosclerosis; Arteriosclerosis; Gamma-carboxyglutamic acid

1. Introduction

In recent years there has been an increasing awareness that 2D cell cultures do not adequately simulate the in vivo condition. This awareness has stimulated a search for new 3D culture methods that mimic this condition. In the period 1997–2005 about 300 papers dealing with 3D cell culture were published and in 2005–2012 ~2000 papers according to PubMed were published. Most of the 3D methods use uniform cell spheroids, a microtiter plate containing uniform histoids, and scaffolds such as hydrogel sponges through which cells can communicate, connect, and move. A significant exception is the 3D culture method using magnetic levitation methodology (MLM). This method allows much faster cell growth and hence performing more experiments per unit time than 2D cultures. MLM has been used successfully with primary lung cells, glioblastoma cells, HUVEC cells, neural stem cells, liver cells, and breast cells. Magnetic levitation culturing is a much improved in vitro cell culturing platform, producing cells that may recapitulate in vivo tissue properties [4]. The applicability of the method to our VSMC system and the accelerated growth rate were important rationales for using MLM in this study. Significantly, cells grown in both cultures produced hydroxy-apatite. There is significant data supporting the view that cells cultured in 2D do retain their phenotypes when grown in 3D (please see Ref [4]). For example glioblastoma cells cultured under 2D and 3D conditions exhibit very similar nuclear and N-cadherin staining patterns.

In previous studies we have demonstrated that when 2D cultures of vascular smooth muscle cells (VSMCs) were treated 12–14 days with 10 nM lyso-phosphatidylcholine (LPC), they underwent transdifferentiation to calcifying vascular cells (CVCs) which form extracellular ridges and extensions containing calcification as indicated by von Kossa and Alizarin Red reagents [1,13–15]. The calcification cascade is controlled by Runx-2, a master transcription factor that modulates the expression of downstream osteogenic proteins. Schnurri-3 has been identified as an inhibitor of Runx-2 in bone differentiation [2,3], suggesting a novel mechanism for controlling the osteoblastic activity of VSMCs in cell cultures. CVCs growing in 2D cultures form extracellular calcified ridges and rods. However, these may not be the most abundant morphologies in 3D calcified tissue. Recently, magnetite beads (*n3D Biosciences*, Houston, TX) have been used to magnetize cells and levitate them in 3D cultures. These 3D cultures grow 3–4 times more rapidly than 2D cultures [4,5], facilitating a detailed study of CVC formation of calcified structures such as nodules and rods.

Recently, we have synthesized a peptide (HABP-19) derived from the α1 region of osteocalcin, having high affinity and specificity for calcium hydroxyapatite. This peptide contains the amino acid sequence βAγEPRRγEVAγELγEPRRγEVAγEL, with the capability

of coupling to a reporter group (e.g., FITC, Cy5.5, etc.) bound to the N-terminus. Its Gla residues enable the peptide to bind to CHA but not to other calcium compounds such as calcium oxalate, calcium carbonate, or calcium pyrophosphate. In this study we have used a fluorescein-conjugated peptide (FITC-HABP-19) to visualize CHA in CVC cultures and to monitor calcification in them [6].

2. Materials and methods

2.1. Tissue processing

Carotid endarterectomy (CEA) tissues were resected from patients undergoing unilateral endarterectomy [7–9]. CEA tissues were collected under a protocol approved by the institutional review board for human research at Baylor College of Medicine. Resected tissues were placed in PBS/glycerol (50/50, v/v) and stored at −20 °C until used.

2.2. Total protein extraction

Cells or calcified tissues were rinsed with cold PBS (3×) and lysed or homogenized with a buffer containing 0.1% octylglucoside plus Ripa Buffer (50/50) (*Thermo Scientific*). The lysate or homogenate was then sonicated for 2 min using an Aquasonic 150HT (*VWR*). Total protein was quantified using the BCA Protein Assay (*Thermo Scientific*, Rockford, IL), per manufacturer's instructions and by Nanodrop™ spectrometry (*Thermo Scientific*).

2.3. Isolation of Schnurri-3

A customized antibody (*GenScript*, Piscataway, NJ) was raised against a synthetic peptide (Shn3-Pep) corresponding to a predicted Schnurri-3 epitope (EEAHKKERKPQKPGKYIC). Anti-Shn3-Pep was isolated from crude antisera by chromatography over Sepharose-Shn3-Pep. The antibody was then coupled to Sepharose to prepare an immunoaffinity column for adsorption of Schnurri-3 protein from the total protein extract from normal regions of human common carotid segments obtained by carotid endarterectomy (CEA).

2.4. Regulation of Schnurri-3

In a separate 2D study we have designed and prepared three siRNAs which provided knockdown efficiencies of 96.7%, 66.2%, and 94.5%. The knockdown of Schnurri-3 was accompanied by significant upregulation of RUNX2, a master transcriptional regulator of osteoblast differentiation, resulting in robust upregulation of osteogenic gene expression (e.g. osteocalcin, collagen, osteopontin, alkaline phosphatase, and osteoprotegerin), (K.C. Vickers, Ph.D. Thesis, 2008, Baylor College of Medicine). An expanded description of that study is the subject of a separate manuscript.

2.5. Magnetic levitation of VSMC 3D cultures

Human aortic smooth muscle cells (PH35405A, *Genlantis*, San Diego, CA) were grown in T-175 flasks. When cells reached ~80% confluency they were transferred to 35 × 10 mm petri dishes. During day zero, cells were treated overnight with MagPLL™, a polylysinebased hydrogel containing gold and magnetite nanoparticles (*n3D Biosciences*, Houston, TX). After cells ingested magnetite nanoparticles they were magnetically levitated

and transferred to 3D cultures using the Bio-Assembler neodymium magnet (*n3D Biosciences*, Houston, TX). Cell viability was determined by the method of Allison et al. [26].

2.6. Determination of calcium, phosphate, and glycosaminoglycans

Calcium was determined by the Arsenazo III reagent (*Pointe Scientific Inc.*, Canton, MI) [1]. Phosphate was measured using Malachite Green (*AnaSpec*, Fremont, CA) [1]; glycosaminoglycan (GAG) (10–12) was quantified by the Blyscan Assay (*Biocolor*, Carrickfergus, UK), according to the manufacturers' instructions. Staining of cell cultures for GAG was performed with Alcian blue reagent (1 g of Alcian blue in 100 ml of 3% acetic acid, pH 2.5). The cell clusters were exposed to the reagent solution for 30 min, then washed in running water for 2 min.

2.7. Inverted microscopy

A Nikon TMS-F inverted microscope was used to acquire cell culture images during four consecutive days in order to document the transformation of VSMCs from 2D to 3D CVC cultures. The day at which the VSMCs had grown to ~80% confluency was designated as day 0.

2.8. Fluorescence detection

2.8.1. On slides—Fluorescence was detected using the inverted microscope present in the laser capture microdissection instrument (Veritas Microdissection Instrument 704, *Arcturus Biosciences Inc*, CA) equipped with a red fluorescence filter cube (Ex/Em 590–650 nm/ >667 nm), a green fluorescence filter cube (Ex/Em 503–547/>565 nm), a blue fluorescence filter cube (Ex/Em 455–495/>510 nm), and a UV fluorescence filter (Ex/Em 340–390/>410 nm). Veritas 2.3 software from the same manufacturer was used. Pellets from each treatment experiment were deposited over pre-cleaned microscope slides (Fisherbrand Superfrost Plus, *Fisher Scientific*, USA).

2.8.2. In microtiter plates—Fluorescence was detected with a Synergy Mx microplate reader using the software Gen5 v1.10.8 (*BioTek*, Winooski, VT).

2.9. Experimental design

The VSMCs were grown in triplicate 3D cultures for each of the following conditions: i) in normal DMEM media + 15% FBS as a negative control; ii) in DMEM media containing 10 nM LPC as a positive control to promote calcification; and iii) in DMEM media containing 10 nM LPC plus 0.5 μg/μl of Schnurri-3 to attenuate calcification.[1].

2.10. Cell viability

VSMC viability was measured with the LIVE/DEAD cell assay described by Alison et al. [27]. A major fraction of cells (~75%) exhibited green fluorescence indicating predominant viability; a minor fraction of the cells (25%) exhibited red fluorescence, indicating cell death.

3. Results

Chemically pure calcium hydroxyapatite (CHA) does not autofluoresce over the wavelength range 340–>667 nm (Fig. 1A), whereas CHA produced by VSMCs which have been treated with LPC and converted to CVCs formed rods/shafts which do autofluoresce over the entire spectral range, especially in the red range (Ex/Em 590– 650/>667 nm) (Fig. 1C). Both of these forms of calcification can be detected by the extrinsic probe, FITC-HABP-19 (Fig. 1B, D). When the probe was added to VSMCs treated with LPC and converted to CVCs, the calcified cell pellet emitted green-yellow fluorescence over the range 455–495/>510 nm (Fig. 1D). Hence the extrinsic fluorescence emitted by a culture treated with the probe can be used to visualize and possibly even quantify CHA in that culture.

Measurements of calcium [1], phosphate [1], and glycosaminoglycans [10–12] were performed on a sample of the suspended cell culture at day 3 (Fig. 2). The results clearly indicated that cells were much more abundant in the LPC-treated osteogenic VSMCs (green) compared to the VSMCs treated with LPC and Schnurri-3 (red), or compared to negative control cells treated with the media alone (blue). When the cells were stained with Alcian blue, they appeared as blue clusters, indicating the presence of GAG. Thin rods extended from the clusters and emitted intense autofluorescence in the UV range (Ex/Em 340–390/ >410 nm) (Fig. 2B).

RUNX2 is the master gene that regulates downstream osteogenic proteins that lead to the formation of calcified structures. Current evidence suggests that Schnurri-3 may modulate RUNX2 levels. Accordingly, we have performed experiments to evaluate the effect ofSchnurri3 on RUNX2 in 2D culture. The treatment of VSMCs with siRNA#1 led to 96.7% knockdown of Schnurri3. This loss of Schnurri3 resulted in a significant up-regulation of RUNX2 (+66%, $p < 0.01$) and of SM22alpha (+50%, $p < 0.01$.) MSX2 and SM alpha actin were not affected by Schnurri3 (Supplementary Fig. 1). These results suggest that the effect of Shnurri-3 depletion on RUNX2 enhancement in 2D culture will also occur in 3D cultures.

VSMCs treatedwith LPC exhibited slow, gradual transdifferentiation and proliferation in 2D culture over a 7 day period (Fig. 3C, green line). When magnetite was added to the culture to the level of 2 μg/ml (low Fe), growth of the 3D culture was enhanced (Fig. 3C, purple line); when the culture was made 200 μg/ml (high Fe) in magnetite, even faster growth was observed as determined by total protein (Fig. 3C, red line). As the VSMCs differentiated into CVCs and began to express an osteogenic phenotype, calcium and phosphate in the media decreased while calcium and phosphate in the CHA pellet increased (Fig. 3A). When Schnurri-3 was added to the media, calcification was attenuated, resulting in minimal changes in cellular calcium and phosphate levels (Fig. 3B). Nevertheless, the observed biochemical changes were attended by morphologic changes (Fig. 3D). Treatment of VSMCs with low level magnetite for one day resulted in low level of magnetite uptake. Increasing the magnetite level resulted in substantial increase in magnetite uptake as reflected in increased formation of dark cell cultures. The abundance of these clusters increased markedly over the next three days, hence the magnetite-mediated 3D culture was very effective in accelerating culture growth. Cultures with the most magnetite were the most dense (Fig. 3D).

The rapid growth of 3D cultures afforded the opportunity for detailed study of the calcification process. A four day experiment was conducted to compare the formation of CHA under 3 different cell culture conditions (Fig. 4): i) media alone (left column), ii) media + LPC (center column), and iii) media + LPC + Schnurri-3 (right column). On day 0 the cells in DMEM were treated with magnetite beads.

By the end of the first day, the control cells had begun to associate with each other and to form random clusters 10–30 μm in diameter with a dark core and bright shell (Fig. 4A). This association was more extensive and organized in cultures treated with LPC which formed multiple spherical clusters (Fig. 4B). The cells treated with both LPC and Schnurri-3 also formed spherical clusters (Fig. 4C).

By the second day, the 3D VSMC culture in media alone displayed remarkable proliferation, showing significantly more cells than typically seen in a 2D culture (Fig. 4D). The cells treated with LPC formed rods extending from interconnected spherical clusters (Fig. 4E). The cells treated with LPC and Schnurri-3 continued proliferating and forming 3D clusters; however these clusters did not form rods or protrusions (Fig. 4F); there was no formation of translucent nodules as were seen only in VSMCs treated with LPC (Fig. 4E). Thus the distinguishing feature of 3D cultures treated with LPC alone was the multiple clustering of spheres and the formation of rod-like structures (Fig. 4E).

On the third day, the cells were moved to a new 35 × 10 mm petri dish containing fresh media. The positive control culture (media + LPC) and the experimental culture (media + LPC + Schnurri-3) exhibited extensive clustering of the spherical groups of cells (Fig. 4H, I).Multiple bright rods were seen in the LPC-treated cultures. These structures were less abundant in the cell culture containing Schnurri-3 treated cells.

On the fourth and final day, the experiment was concluded. The VSMCs that were maintained on normal media continued to remain associated (Fig. 4J). The VSMCs treated with LPC formed a dense cellular network and a chain of multiple beads or nodules. The VSMC culture treated with both LPC and Schnurri3 formed longer and thinner rods/and shafts (Fig. 4L). Hence, the clustering of cells and the formation of rod shaped structures appeared to be enhanced by LPC and attenuated by Schnurri-3 in these cultures.

These results suggest that in the 3D culture system, cell clusters form and extrude rod-like structures (Fig. 4E, H, L). These rods contain hydroxyapatite as indicated by the yellow-green fluorescence from FITC-HABP-19 which binds specifically to hydroxyapatite (Fig. 4N,O). A macro-cluster of CVCs stained with Alcian blue demonstrated the presence of GAG (Fig. 2B, upper). Hence it appears that CVCs have the capability of extracting calcium and phosphate from the medium and creating local concentrations sufficient to exceed the Ksp for hydroxyapatite. This process may be accelerated by osteogenic proteins which serve as a structural matrix.

4. Discussion

When eighty percent confluent vascular smooth muscle cells (VSMCs) were incubated overnight with gold/magnetite particles, magnetically levitated 3D cultures were obtained

which appeared as free standing and clustered cells that proliferated 3–4 times faster than cells in conventional 2D cultures. When cells labeled with magnetic nanoparticles were incubated with media containing LPC, cell clusters 250–625 μm in diameter exhibited translucent extensions/ rods 95–150 μm wide and up to 1250 μm long. When Schnurri-3 was added to the 3D culture containing LPC, these rods were smaller or absent. When excited with 590–650 nm light, these rods emitted intrinsic fluorescence at >667 nm. When the 3D cultures were treated with a FITC-conjugated fluorescent probe specific for calcium hydroxyapatite (FITC-HABP-19), the cell rods emitted intensely at 518 nm, the FITC λ-max. Cell culture pellets were enriched in calcium, phosphate, and glycosaminoglycans (GAGs).

The size and shape of the calcified structures are informative. The cylindrical rods formed by 3D cultures of VSMC stand in contrast to the calcified spherical granules and flat plates formed in atherosclerotic lesions [24,29]. Extracellular calcified granules are in part, structures that initially form intracellularly and then are released after cell death. Extracellular calcification from cell remnants then combine and grow to form larger structures. In this study the calcified rods varied in size, depending on the culture media content. They ranged up to 125 μm in width and 1250 μm in length, dimensions not normally accommodated by SMCs. This suggests that calcified rod formation may begin in the cell where adequate amounts of calcium and phosphate can be stored to initiate calcification. As the rod is formed, it may be extruded into the extracellular space. The availability of osteogenic proteins, which is controlled by RUNX2 and Schnurri-3, may play an important role in rod formation and extrusion.

Inorganic hydroxyapatite does not emit autofluorescence, as compared to the “organic hydroxyapatite” produced by VSMCs when treated with LPC. Some investigators ascribe the origin of autofluorescence in bone to the presence of unidentified osteoid/osteoclast proteins [17,18]. Teeth have been reported to exhibit a higher autofluorescence in specific sites corresponding to osteocytes, osteoblasts, and osteoid matrix [19]. Calcified CEA tissues [25] exhibit considerable autofluorescence which can be used to distinguish calcified from non-calcified zones [16]. When these tissues are subjected to total protein extraction, their autofluorescence is significantly reduced. The protein(s) that bind to calcified sites and confer autofluorescence on them are currently under investigation.

The level of Runx-2, the master regulator of bone mineralization, is controlled by Schnurri-3, which promotes Runx2 degradation in the proteasome [2,3]. Recently, the Snail-1 protein was found to be a transcriptional effector of FGFR3, thereby regulating longitudinal bone growth [19,20]. Snail-1 is the first reported transcriptional repressor of Runx-2 [20,21]. Snail-1 transcriptional control, together with the translational [22] and post-translational regulation of RUNX2, effected by Twist [23] and Schnurri-3 [2,3], orchestrates the complex dynamics of protein activity during osteoblast differentiation. The present study demonstrates the capacity of Schnurri-3 to attenuate calcification. In a culture of VSMC + LPC, CHA rods 208–258 μm long are formed, whereas when the culture contained VSMC + LPC + Schnurri-3, the rod length was reduced to 50–124 μm. We anticipate a similar mechanism for regulation of Runx-2 during vascular calcification.

A pivotal event in the beginning of VSMC calcification is the release of mineralization competent matrix vesicles (MV), small membrane bound particles with structural features enabling them to efficiently nucleate hydroxyapatite [28]. As these vesicles mature, their amorphous Ca/P becomes organized into structured Octa Ca/P, and finally to calcium/hydroxyapatite which emerges as rod-like structures. Matrix vesicle biogenesis occurs by polarized budding and pinching off of vesicles from specific regions of the outer plasma membranes of differentiating growth plate chondrocytes, osteoblasts, and odontoblasts. Polarized release of MVs into selected areas of developing matrix determines the non-random distribution of calcification [29]. Some of the structures found in the 3D VSMC cultures resemble structures seen in 2D osteoblast cultures. The beads/nodules seen in Fig. 4K resemble matrix vesicles enriched in Ca/P. The fluorescent rods seen in Fig. 4N, O are suggestive of the filaments secreted by matrix vesicles. Significantly, the calcified structures seen in our 3D cultures are almost always attached to cells or cell clusters (Figs. 2B, 4E,H,K), providing evidence that the formation of apatite in VSMC cultures is not the result of passive precipitation, but rather the outcome of cell-mediated formation. It appears that GAGs also play an important role in 3D osteogenesis, given its greater abundance than calcium and phosphate, and its direct association with calcified rods (Fig. 2A,B). Its role in calcified aortic and mitral valves is currently under investigation.

VSMCs avidly phagocytized magnetite beads, enabling the cells to levitate in a 3D culture. The levitated cells proliferated more rapidly and associated more extensively than in 2D cultures of cells containing no magnetite. 2D and 3D cells treated with LPC showed thick, intensely autofluorescent, and long calcified formations, while the cells treated with both LPC and Schnurri-3 were fewer and thinner, and exhibited weakly autofluorescent calcified formations. The CHA in these formations can now be detected using a novel, highly sensitive probe, FITC-HABP-19. 3D culture technology affords important advantages in the study of VSMCs. Additional advantages have been reported for 3D cultures of other cell types [4,5]. The formation of calcified structures in 3D VSMC cultures suggests that similar structures may be formed in vivo. The results of this study suggest a mechanism for attenuating calcification in other relevant cell types, animal models, and man.

Accumulating evidence suggests that in the 3D system, cell clusters form and extrude rod-like structures (Fig. 4E, H, L). These rods contain hydroxyapatite as indicated by the yellow-green fluorescence from FITC-HABP-19 which binds specifically to hydroxyapatite (Fig. 4N,O). A macro-cluster of CVCs stained with Alcian blue demonstrated the presence of GAG (Fig. 2B, upper). Hence it appears that CVCs have the capability of extracting calcium and phosphate from the medium and creating local concentrations sufficient to exceed the Ksp for hydroxyapatite. This process may be accelerated by osteogenic proteins which serve as a structural matrix.

Supplementary Material

Refer to Web version on PubMed Central for supplementary material.

Acknowledgements

This study was supported in part by HL-63090 and HL-07812. The authors are indebted to: Iou Chen for the technical assistance; Glauco Souza for the n3D Beta Test; and Michael Reardon and Alan Lumsden for providing the CEA tissues (TTGA).

Abbreviations

CHA	calcium hydroxyapatite
LPC	lysophosphatidylcholine
VSMC	vascular smooth muscle cell
CVC	calcifying vascular cell
HABP-19	hydroxyapatite binding peptide containing 19 amino acids
CEA	carotid endarterectomy
Ca/P	calcium/phosphorus
FBS	fetal bovine serum
Shn3	Schnurri-3; PO, phosphate
GAG	glycosaminoglycan
FITC	fluoroscein isothiocyanate
Gla γE	gamma-carboxy glutamic acid
βA	beta alanine
MLM	magnetic levitation

References

1. Vickers KC, Castro-Chavez F, Morrisett JD. Lyso-phosphatidylcholine induces osteogenic gene expression and phenotype in vascular smooth muscle cells. Atherosclerosis. 2010; 211:122–129. [PubMed: 20451909]
2. Jones DC, Wein MN, Oukka M, Hofstaetter JG, Glimcher MG, Glimcher LH. Regulation of adult bone mass by the zinc finger adapter protein Schnurri-3. Science. 2006; 312:1223–1227. [PubMed: 16728642]
3. Jones DC, Schweitzer MN, Wein M, Sigrist K, Takagi T, Ishii S, Glimcher LH. Uncoupling of growth plate maturation and bone formation in mice lacking both Schnurri-2 and Schnurri-3. Proc. Natl. Acad. Sci. U. S. A. 2010; 107:8254–8258. [PubMed: 20404140]
4. Souza GR, Molina JR, Raphael RM, Ozawa MG, Stark DJ, Levin CS, Bronk LF, Ananta JS. Three-dimensional tissue culture based on magnetic cell levitation. Nat. Nanotechnol. 2010; 5:291–296. [PubMed: 20228788]
5. Molina J, Hayashi Y, Stephens C, Georgescu MM. Invasive glioblastoma cells acquire stemness and increased Akt activation. Neoplasia. 2010; 12:453–463. [PubMed: 20563248]
6. Lee JS, Tung CH. Osteocalcin biomimic recognizes bone hydroxyapatite. Chem Bio Chem. 2011; 12:1669–1673.
7. Castro-Chavez F, Morrisett JD. Osteogenic transdifferentiation of vascular smooth muscle cells to calcifying vascular cells I 3D culture: enhancement by lyso-phosphatidylcholine and attenuation by Schnurri-3, Poster 1108-116, ACC 11. J. Am. Coll. Cardiol. 2011; 57:E1548. (Abs).

8. Ennix CL, Lawrie GM, Morris GC, Crawford ES, Howell JF, Reardon MJ, Weatherford SC. Improved results of carotid endarterectomy in patients with symptomatic coronary disease: an analysis of 1,546 consecutive carotid operations. Stroke. 1979; 10:122–125. [PubMed: 312551]
9. Stove J, Schneider-Wald B, Scharf HP, Schwarz ML. Bone morphogenetic protein 7 (bmp-7) stimulates proteoglycan synthesis in human osteoarthritic chondrocytes in vitro. Biomed. Pharmacother. 2006; 60:639–643. [PubMed: 17056223]
10. Duer MJ, Friscic T, Proudfoot D, Reid DG, Schoppet M, Shanahan CM, Skepper JN, Wise ER. Mineral surface in calcified plaque is like that of bone: further evidence for regulated mineralization. Arterioscler. Thromb. Vasc. Biol. 2008; 28:2030–2034. [PubMed: 18703777]
11. Demer LL, Sage AP, Tintut Y. Nanoscale architecture in atherosclerotic calcification. Arterioscler. Thromb. Vasc. Biol. 2008; 28:1882–1884. [PubMed: 18946051]
12. Kougias P, Chai H, Lin PH, Lumsden AB, Yao Q, Chen C. Lysophosphatidylcholine and secretory phospholipase A2 in vascular disease: mediators of endothelial dysfunction and atherosclerosis. Med. Sci. Monit. 2006; 12:RA5–RA16. [PubMed: 16369478]
13. Matsumoto T, Kobayashi T, Kamata K. Role of lysophosphatidylcholine (LPC) in atherosclerosis. Curr. Med. Chem. 2007; 14:3209–3220. [PubMed: 18220755]
14. Schmitz G, Ruebsaamen K. Metabolism and atherogenic disease association of lysophosphatidylcholine. Atherosclerosis. 2010; 208:10–18. [PubMed: 19570538]
15. Vickers, KC. Ph.D. Thesis. Houston, TX: Baylor College of Medicine; 2008. Integrated investigation of low density lipoprotein modifications, lipoprotein-associated phospholipase A2, and vascular smooth muscle cell osteogenic trans-differentiation in human atherosclerosis and vascular calcification; p. 1-453.
16. Capasso L, D'Anastasio R, Michetti E. The use of the confocal microscope in the study of ancient human bones. l'Anthropologie. 2001; 39:181–186.
17. Piattelli A, Trisi P. Bone ingrowth into hydroxyapatite coating: a light microscopy and laser scanning microscopy study. Biomaterials. 1993; 14:973–977. [PubMed: 8286675]
18. de Frutos CA, Vega S, Manzanares M. Snail is a transcriptional effector of FGFR3 signaling during chondrogenesis and achondroplasias. Dev. Cell. 2007; 13:872–883. [PubMed: 18061568]
19. de Frutos CA, Dacquin R, Vega S, Jurdic P, Machuca-Gayet I, Nieto MA. Snail-1 controls bone mass by regulating Runx2 and VDR expression during osteoblast differentiation. EMBO J. 2009; 28:686–696. [PubMed: 19197242]
20. Park SJ, Jung SH, Jogeswar G. The transcription factor Snail regulates osteogenic differentiation by repressing Runx2 expression. Bone. 2010; 46:1498–1507. [PubMed: 20215006]
21. Huang J, Zhao L, Xing L, Chen D. MicroRNA-204 regulates Runx2 protein expression and mesenchymal progenitor cell differentiation. Stem Cells. 2010; 28:357–364. [PubMed: 20039258]
22. Bialek P, Kern B, Yang X. A twist code determines the onset of osteoblast differentiation. Dev. Cell. 2004; 6:423–435. [PubMed: 15030764]
23. Saita Y, Takagi T, Kitahara K. Lack of Schnurri-2 expression associates with reduced bone remodeling and osteopenia. J Biol Chem. 2007; 282:12907–12915. [PubMed: 17311925]
24. Hunt JL, Fairman R, Mitchell ME. Bone formation in carotid plaques: a clinicopathological study. Stroke. 2002; 33:1214–1219. [PubMed: 11988593]
25. Lee JS, Morrisett JD, Tung C-H. Detection of hydroxyapatite in calcified cardiovascular tissues. Atherosclerosis. 2012; 224:340–347. [PubMed: 22877867]
26. Alison DD, Drazba JA, Vesely I, Kader KN, Grande-Allen KJ. Cell viability mapping within long term heart valve organ cultures. J Heart Valve Dis. 2004; 13:290–296. [PubMed: 15086269]
27. Kapustin AN, Shanahan CM. Calcium regulation of vascular smooth muscle cell derived matrix vesicles. Trends Cardiovasc. Med. 2012; 22:133–137. [PubMed: 22902179]
28. Anderson HC. Matrix vesicles and calcification. Curr. Rheumatol. Rep. 2003; 5:222–226. [PubMed: 12744815]
29. Stary HC. Natural history of calcium deposits in atherosclerosis progression and regression. Z. Kardiol. 2000; 89(Suppl. 2):II28–II35.

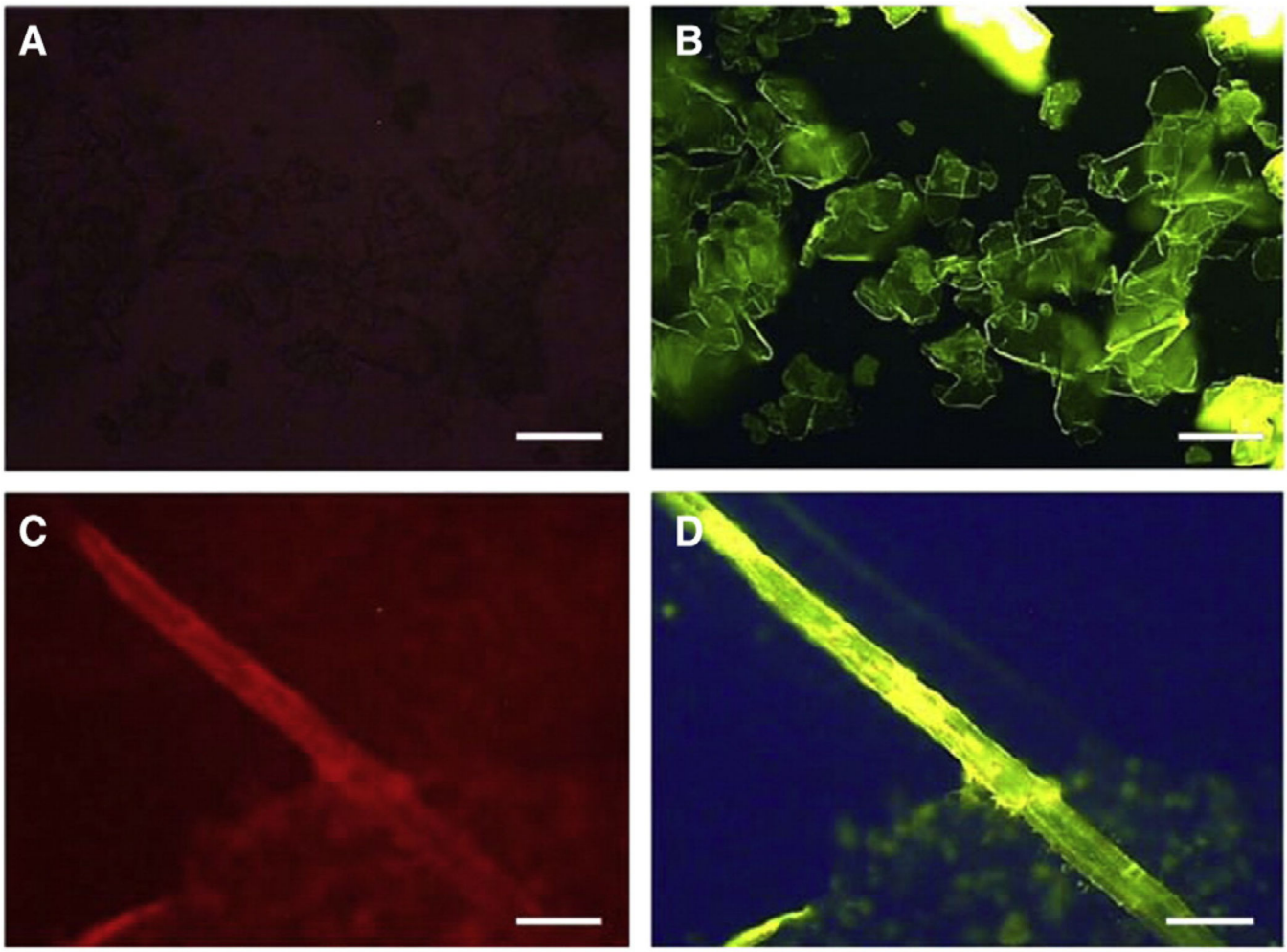

Fig. 1.

Calcification visualization by FITC-HABP-19. (A) Non-fluorescence of inorganic HA. (B) Extrinsic fluorescence of HA in 410 to >565 nm range when treated with FITC-HABP-19. (C) Intrinsic fluorescence of HA formed in cell culture through the spectral range 410 to >667 nm, especially in the red range. (D) Fluorescence of biologically produced hydroxyapatite with the FITC-HABP-19 probe. [A–D (40×), scale bars = 250 μm].

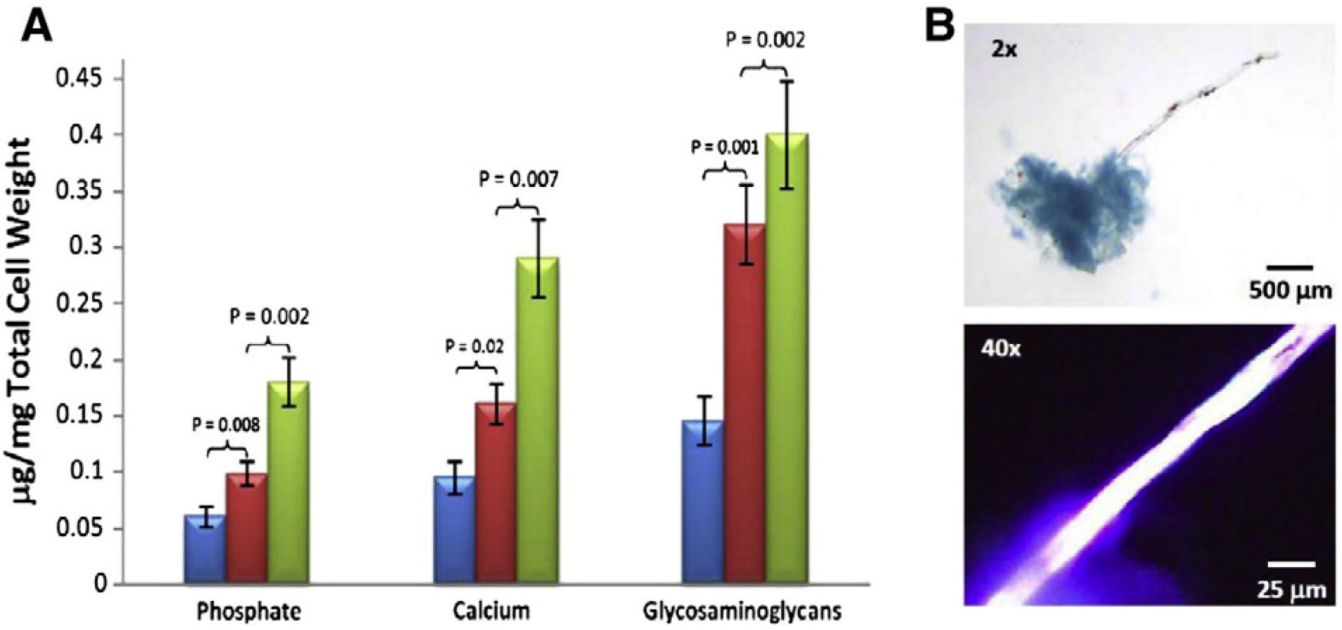

Fig. 2.

Comparison of phosphate, calcium and glycosaminoglycans in VSMCs cultured in the presence (+) or absence (−) of LPC or Schnurri-3. (A) The blue histograms represent the VSMCs in the DMEM media without LPC or Schnurri-3. The red histograms represent the VSMCs with LPC and Schnurri-3. The green histograms represent the VSMCs with LPC but without Schnurri-3. (B) A cluster of CVCs stained with Alcian Blue demonstrating the presence of GAGs (upper image), and the intrinsic fluorescence of a calcified rod (Ex/Em 340–390/>410 nm) (lower image).

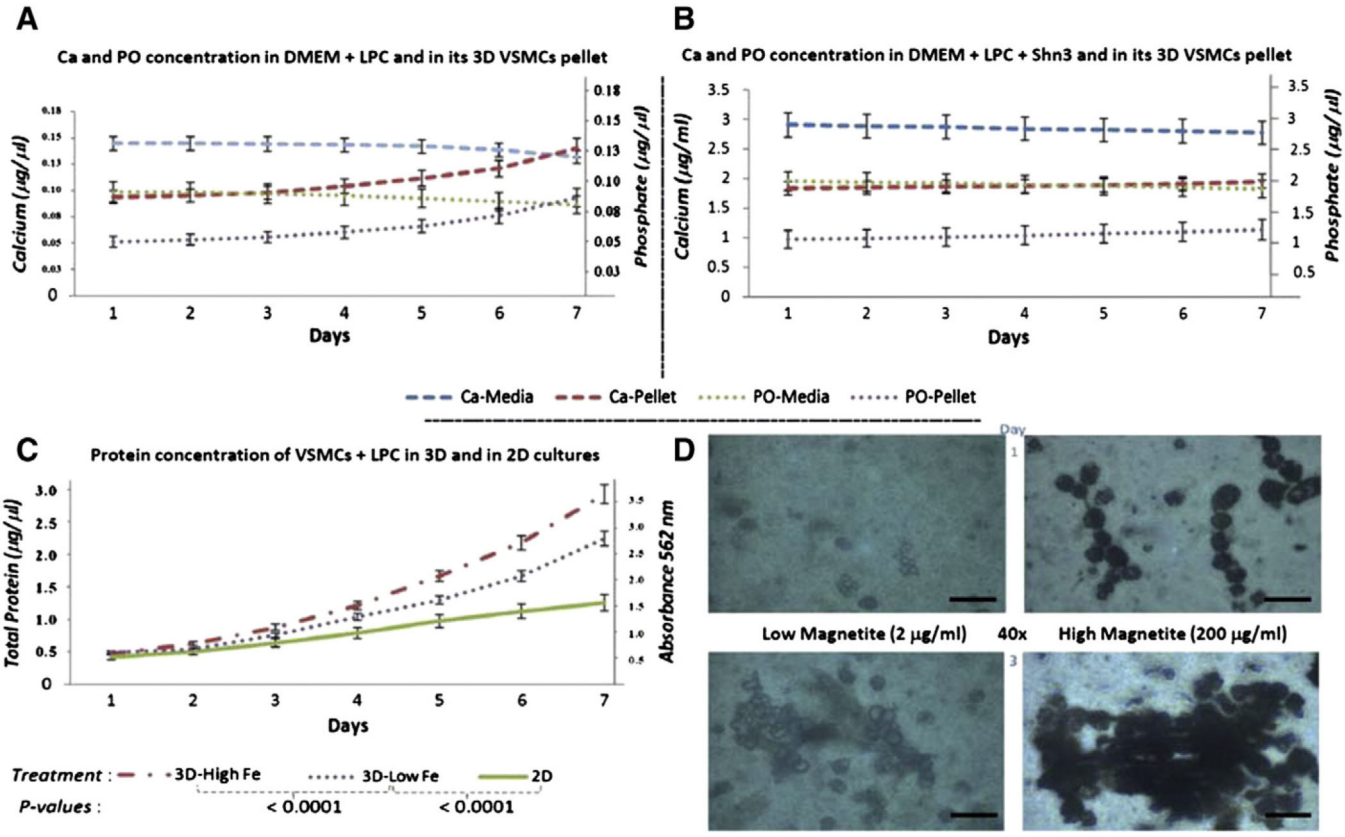

Fig. 3.

Comparison of calcium and phosphate in VSMCs in the absence or presence of Schnurri-3 and in two magnetite concentrations. (A) Calcium and phosphate in the absence of Schnurri-3 decrease in the media while increasing in the cells. Calcium was measured by Arsenazo III (*Pointe Scientific*) at an absorbance of 650 nm. PO was measured by Malachite green (*AnaSpec*) at an absorbance of 635 nm. (B) Calcium and phosphate in the presence of Schnurri-3 do not show a change between media and cells. (C) Total protein content by BCA analysis in 2D or 3D under low or high magnetite (3D-Low Fe vs 3D-High Fe, respectively). (D) Comparison of the low vs high magnetite concentrations as viewed by inverted microscopy (scale bars = 25 µm); increasing the magnetite concentration enhanced the growth of 3D cultures of VSMCs.

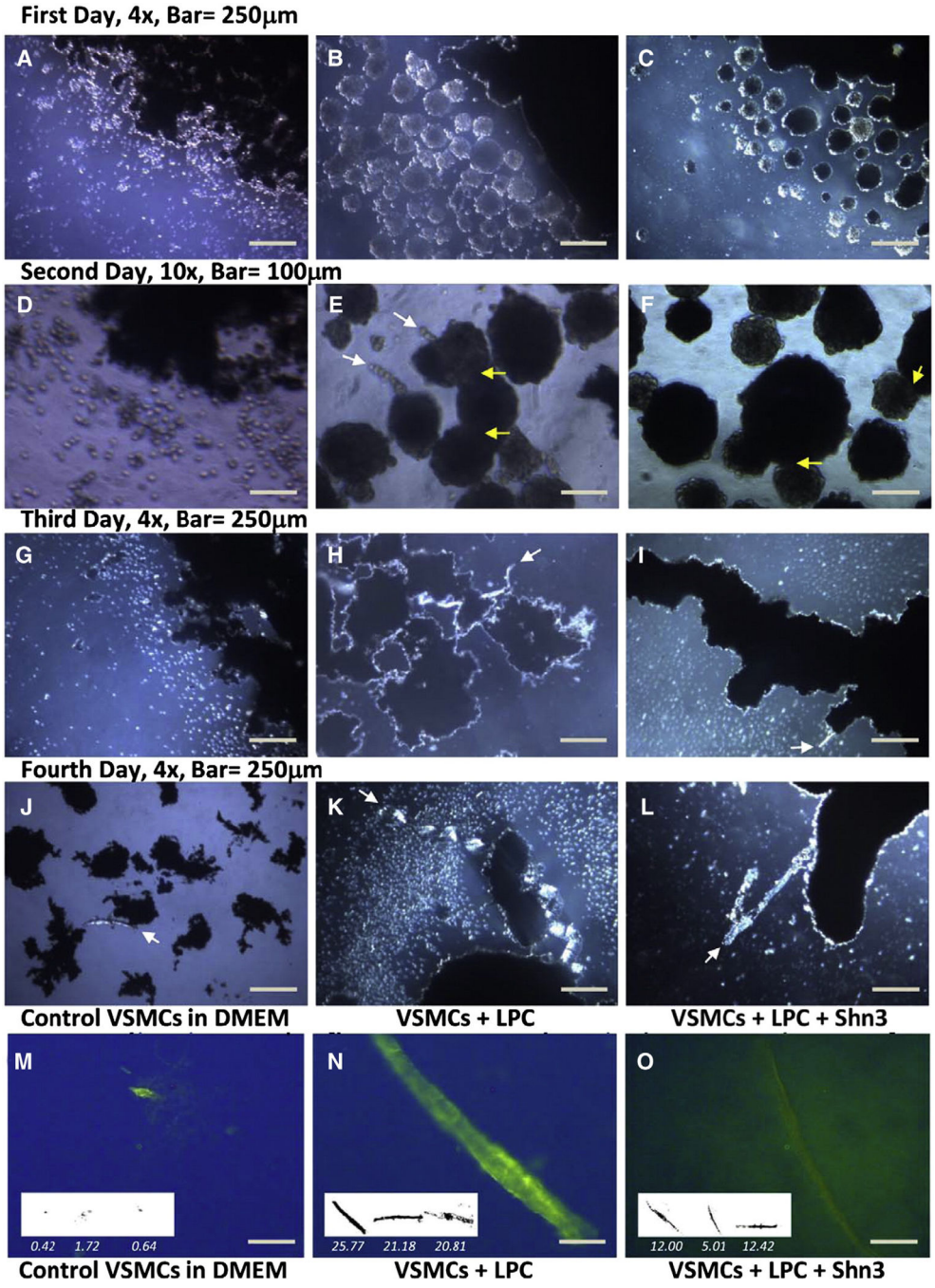

Fig. 4.

A four day serial culture of 3D VSMCs: In media alone (left column: A, D, G, J). In media + LPC (center column: B, E, H, K). In media + LPC + Schnurri-3 (right column: C, F, I, L). Images A–L were acquired under bright field illumination. Yellow arrows indicate some of the cell cluster fusion points; white arrows indicate incipient calcification (HA). Strands of calcified nodules are seen in panel K and thin calcified rods are present in panel L. Treatment of the fourth day culture with HABP-19 resulted in localization of green

fluorescence (570 nm) to rods of HA (Images N, O). Scale bar = 250 μm. Inserts show calcified rods with lengths divided by factor of 10.